INTERNATIONAL JOURNAL OF
COASTAL, OFFSHORE & ENVIRONMENTAL ENGINEERING IJCOE Vol.11 /No.1 /Winter 2026 (34-45)

Available online at: www. ijcoe.org

Numerical Modeling and Hydrodynamic Sensitivity Analysis of Storm Surge in the Southern Caspian Sea: The Role of Bathymetry and Wind Stress

Mahmood Reza Akbarpour Jannat[1*]; Abbas Hamidi Najafabadi[2]

[1]Iranian National Institute for Oceanography and Atmospheric Science, No.3, Etemad Zadeh St., Fatemi Ave, P.C: 1411813389, Tehran, Iran, E-mail: akbarpour@inio.ac.ir*
[2]M.Sc. Graduate, Department of Marine Engineering, Science and Research Branch, Islamic Azad University, Tehran, Iran. E-mail: abbass_hamidi@yahoo.com

ARTICLE INFO

Article History:
Received: 17 Aug 2025
Accepted: 17 Dec 2025

Keywords:
Storm Surge
ADCIRC
Southern Caspian Sea
Wind Shear Stress
Coastal Hydrodynamics

ABSTRACT

The precise estimation of extreme water level fluctuations induced by storm surges constitutes a fundamental prerequisite for the reliable design of marine structures and effective coastal risk management. In this study, the hydrodynamic response of the Southern Caspian Sea coast to atmospheric forcing mechanisms is investigated using the advanced ADCIRC numerical model, employing the solution of Shallow Water Equations (SWE) over an unstructured finite element mesh. To conduct a rigorous spatial and parametric sensitivity analysis, simulations were executed under various wind field and atmospheric pressure scenarios across six strategic stations characterized by distinct morphological features, ranging from the shallow waters of Gomishan to the steep bathymetry of Astara. Quantitative results substantiate a distinct non-linear inverse correlation between the seabed depth gradient and surge amplitude; specifically, the southeastern coasts experience surge magnitudes of a higher order compared to the steep western coasts, attributed to the continental shelf geometry and the momentum trapping phenomenon. Furthermore, the decoupling of driving forces reveals that water level variations within the Caspian basin are predominantly governed by the wind shear stress vector and effective fetch, with the inverse barometric effect playing a secondary role. By elucidating the spatial heterogeneity of coastal risks—inundation hazards in the east versus wave impact loads in the west—the findings provide a novel framework for determining the Design Water Level (DWL) and calculating hydrodynamic loads on offshore piles and protective seawalls.

1. Introduction

The sustainable development of coastal zones and the assurance of the structural integrity of critical infrastructure including ports, power plants, and offshore platforms are intrinsically linked to a precise understanding of the complex interactions between the atmosphere and the ocean. One of the most challenging parameters in the design of hydraulic structures is the determination of the "Design Water Level" (DWL).

While the water level is typically conceptualized as the superposition of Mean Sea Level (MSL), astronomical tides, and surge, in the context of extreme events, the "Storm Surge" phenomenon emerges as the dominant governing factor in short-term water level fluctuations. Neglecting the nonlinear and dynamic nature of this phenomenon can lead to gross errors in estimating the crest elevation of breakwaters and hydrodynamic loads on platform piles, ultimately resulting in catastrophic structural failure or severe inundation of the hinterland (Mahdizadeh, 2004).

From a hydrodynamic perspective, storm surge represents the response of the water body to meteorological forcing mechanisms, primarily comprising Wind Stress and atmospheric pressure gradients. When high-velocity wind fields blow over the sea surface with sufficient duration, the induced

shear stress facilitates momentum transfer to the surface layers, resulting in water pile-up in the direction of the wind (Wind Setup). Concurrently, the pressure deficit at the center of low-pressure systems leads to a rise in the sea surface via the Inverse Barometric Effect. The magnitude and amplitude of this phenomenon are complex functions of the wind field characteristics, the Coriolis effect due to latitude, coastal geometry, and, critically, the seabed morphology (Bathymetry) (Williams, 1986). Classical principles of coastal hydraulics dictate that in shallow waters, the potential for surge generation amplifies significantly due to the reduced return flow area and increased bottom friction a fact that underscores the absolute necessity of site-specific studies.

The Caspian Sea, as the world's largest enclosed body of water, serves as a unique natural laboratory for studying hydrodynamic phenomena. Lacking connection to the open oceans, its astronomical tidal range is negligible (micro-tidal). Consequently, short-term water level fluctuations within this basin are almost exclusively governed by atmospheric forces and storm surges. Historical records and observational data indicate that the Caspian Sea is prone to severe storms with long return periods. The severe heterogeneity in seabed topography ranging from the extremely shallow northern sector to the deep southern basin dictates a dual behavior for storm surges. While extensive studies have focused on massive 4–5 meter surges in the Northern Caspian (Mahdizadeh, 2004), the hydrodynamics of the Southern Caspian Basin (bordering Iran), characterized by a narrower continental shelf and greater depths, have been less rigorously scrutinized. However, the historical record of the November 1910 storm, which generated a surge of approximately 2 meters under easterly winds of 20–26 m/s, corroborates the high hazard potential in this region (Wu, 1982).

In recent decades, with the rapid expansion of strategic infrastructure along the southern coastline (including the ports of Anzali, Nowshahr, and Amirabad, as well as oil facilities), reliance on traditional methods and one-dimensional empirical formulas for surge estimation is no longer sufficient for modern engineering requirements. These conventional approaches fail to resolve current refraction, spatial variability of wind fields, and the complexities of the coastline. Therefore, the deployment of advanced numerical hydrodynamic models that solve the Shallow Water Equations (SWE) over refined computational grids is inevitable (Yan, 1987).

The present research is formulated to bridge the existing knowledge gap regarding the hydrodynamics of the Southern Caspian coast. In this study, the ADCIRC (Advanced Circulation) model, based on the Finite Element Method (FEM), is utilized for the two-dimensional simulation of flow and water levels (Luettich and Westerink, 2004). The distinctive approach of this study extends beyond mere simulation; we conduct a rigorous sensitivity analysis of the basin's response to parameters including "Wind Direction," "Atmospheric Pressure," and "Bathymetry" across six key stations with distinct morphological characteristics (ranging from the shallow waters of Gomishan to the deeper coast of Astara). Furthermore, a novel aspect of this research lies in coupling the model's hydrodynamic outputs with structural design equations, where the effects of wave-current interaction and surge-induced water level rise on the forces exerted on marine piles and seawalls are quantitatively evaluated (Karami Khaniki, 2006). The findings of this investigation provide profound insights for optimizing structural design and enhancing risk management strategies in the Southern Caspian Sea.

2. Theoretical Framework, Mathematical Formulation, and Numerical Solution Method

Developing a reliable numerical model for storm surge prediction necessitates a profound understanding of the physical mechanisms governing long-wave generation and propagation. This section first examines the system's behavior under limit states using analytical solutions to provide necessary physical insight. Subsequently, the numerical solution algorithm for the Shallow Water Equations (SWE) is elucidated, and finally, the mathematical framework for calculating hydrodynamic loading on marine structures is presented.

2.1 Asymptotic Behavior Analysis: Steady State and Wind Stress

To isolate the effect of **Wind Stress** as the dominant forcing agent in the Caspian Sea, an idealized channel with uniform depth d and finite length is initially considered. Assuming the system has reached a steady state and the net flow within the channel is zero ($M=0$), the linearized momentum balance equation, neglecting Coriolis effects and advective accelerations, can be expressed as (Williams, 1986):

$$\rho_w g(d+\zeta)\frac{d}{dx}(\zeta-\zeta_\circ)=\tau_s-\tau_b \qquad (1)$$

In this relationship, the water surface gradient ($d\zeta/dx$) directly counteracts the surface wind shear stress (τ_s) and the bottom friction stress (τ_b). Adopting the conventional assumption of a linear relationship between bottom and surface stresses ($\tau_b = -k\tau_s$), where k is the bottom calibration coefficient, Eq. (1) is rewritten as:

$$\tau_b=-5\gamma_b\tau_s=-k\tau_s \qquad (2)$$

By substituting and integrating over the spatial domain, and assuming that water level variations are negligible

compared to the total depth ($d \gg \zeta$), the analytical expression for the surge profile is obtained:

$$\frac{d}{dx}(\zeta - \zeta_{\circ}) = \frac{(1+k)\tau_s}{\rho_w g d} = \frac{(1+k)\rho_a \gamma_s^2}{\rho_w g d} U^2 \tag{3}$$

$$\zeta = \zeta_{\circ} + k \int_{xo}^{x} U^2 dx, k = (1+k)\frac{\rho_a \gamma_s^2}{\rho_w g d} \tag{4}$$

Equation (4), a generalized form of Colding's Formula, demonstrates that surge height is inversely proportional to water depth (d). This physical reality justifies the extreme vulnerability of the shallow southeastern Caspian coasts (e.g., Gomishan) compared to the deep western coasts.

2.2. Wave Dynamics and Proudman Resonance

The second factor driving storm surge is atmospheric pressure variation. The sea surface response to a moving low-pressure center with velocity V can lead to resonance phenomena. By modeling the pressure function as a traveling disturbance $\zeta_0 = -F(t-x/V)$ and solving the unsteady continuity and momentum equations (Wu, 1982):

$$\begin{aligned} \frac{\partial M}{\partial t} &= -gd\frac{\partial}{\partial x}(\zeta - \zeta_{\circ}) \\ \frac{\partial \zeta}{\partial t} &= -\frac{\partial M}{\partial x} \end{aligned} \tag{5}$$

The governing wave equation for the system is derived:

$$\frac{\partial^2 M}{\partial t^2} - gd\frac{\partial^2 M}{\partial x^2} = gd\frac{\partial^2 \zeta_{\circ}}{\partial x \partial t} \tag{6}$$

The analytical solution to this partial differential equation reveals the system's strong dependence on the wave Froude number ($F_r = V/c$), where $c = \sqrt{gd}$ is the shallow-water wave celerity:

$$\begin{aligned} M &= \frac{Vc^2}{C^2 - V^2}\left[F(t - \frac{x}{V}) - F(t + \frac{x}{c})\right] \\ \zeta &= \frac{c}{c^2 - V^2}\left[cF(t - \frac{x}{V}) + VF(t + \frac{x}{c})\right] \\ C &\equiv \sqrt{gd} \end{aligned} \tag{7}$$

Analysis of this relationship reveals three distinct behavioral regimes:

1. Sub-critical Regime ($V < c$): The system response is stable.
2. Resonance Regime ($V = c$): Continuous energy transfer occurs from the atmosphere to the ocean, and the wave amplitude approaches infinity (mathematical singularity). This phenomenon, known as Proudman Resonance, can lead to destructive rogue surges in regions of the Caspian Sea where the storm propagation speed matches the shallow water wave speed.
3. Super-critical Regime ($V > c$): The system undergoes a phase shift, resulting in a negative response (set-down).

2.3. Numerical Solution Strategy: Spatio-Temporal Discretization

To accurately simulate non-linear interactions within the complex geometry of the Caspian Sea, numerical methods are indispensable. The solution algorithm is based on discretizing the governing equations ($\partial f/\partial t = F$) using a central difference (Leap-Frog) scheme, which provides second-order temporal accuracy (Yan, 1987; Luettich and Westerink, 2004:

$$f_{n+1} = f_{n-1} + 2F_n \Delta t \tag{8}$$

Applying this scheme to the full momentum and continuity equations (incorporating Coriolis and surface stress terms), the discrete form on the computational grid (i ,j)is derived:

$$\begin{aligned} \frac{\partial M}{\partial t} &= -gd\frac{\partial}{\partial x}(\zeta - \zeta_{\circ}) + \tau_S{}^{(x)} \\ \frac{\partial N}{\partial t} &= -gd\frac{\partial}{\partial y}(\zeta - \zeta_{\circ}) + \tau_S{}^{(y)} \\ \frac{\partial \zeta}{\partial t} &= \frac{\partial M}{\partial x} - \frac{\partial N}{\partial y} \end{aligned} \tag{9}$$

This method allows for the step-by-step simulation of the temporal evolution of the water surface (ζ) and flow fields (M, N) under various storm scenarios.

2.4. Implications for Marine Structural Design and Integrity Assessment

Although the primary objective of this research is centered on hydrodynamic simulation, the derived model outputs—specifically the spatiotemporal evolution of water surface elevation (ζ) and the associated current velocity fields constitute the fundamental "Hydrodynamic Boundary Conditions" for the design and reliability assessment of coastal infrastructure. The storm-induced rise in the mean water level is not merely a static addition; it effectively augments the total water depth at the toe of coastal structures ($d_{total}=d_{MSL}+\zeta_{surge}+\zeta_{wave\_setup}$). This depth modulation fundamentally alters the wave-

structure interaction regime, shifting the design parameters from standard operational conditions to critical Ultimate Limit States (ULS).

2.4.1. Effects on Slender, Pile-Supported Structures

For pile-supported structures such as offshore platforms, jetties, and dolphins, the surge-induced increase in water depth has a cascading effect on hydrodynamic loading. According to the principles of the Morison Equation, the total force is a summation of drag and inertia components. The surge elevation extends the wetted length of the pile, thereby exposing a larger surface area to hydrodynamic stress. More critically, the increase in depth modifies the wave kinematics; it reduces the attenuation of orbital particle velocities near the surface. Consequently, the structure is subjected to higher velocities at higher elevations. This upward shift of the force center significantly increases the "overturning moment" at the mudline (seabed), which is often the governing failure mode for pile foundations. Therefore, neglecting the surge component can lead to a severe underestimation of the lever arm and the resulting bending moments.

2.4.2. Impact on Gravity Structures (Seawalls and Breakwaters)

In the context of gravity-based coastal defense structures like vertical seawalls and rubble-mound breakwaters, the implications of storm surge are even more decisive. The stability of these structures is governed by the dynamic pressure distribution, typically calculated using methods such as Goda's Theory. The depth-limited wave breaking criterion ($H_{max} \approx 0.78 d_{total}$) dictates that the maximum wave height capable of reaching a structure is a function of the local depth.

During a surge event, the deepened water column mitigates or delays wave breaking on the foreshore. This phenomenon allows larger, high-energy waves which would otherwise break and dissipate energy offshore to propagate closer to the coast and impact the structure directly. This shift can transition the loading regime from a "pulsating" (non-breaking) load to a catastrophic "impulsive" (breaking/shock) load, exerting extreme instantaneous pressures on the wall. Furthermore, the elevated water level significantly increases the risk of "Wave Overtopping," threatening the structural integrity of the crest and the safety of the hinterland. Thus, integrating the computed surge values into the "Design Water Level" (DWL) is indispensable for ensuring structural resilience and preventing functional failure during extreme events.

3. Study Area and Environmental Characterization

3.1. Physiography and Hydrodynamic Characteristics of the Southern Caspian Basin

The Caspian Sea, distinguished as the world's largest endorheic (landlocked) body of water, constitutes a unique hydrodynamic laboratory where the conventional drivers of oceanic variability are fundamentally altered. Unlike open oceans where astronomical tides often dictate coastal water levels, the Caspian Sea functions as a non-tidal system (micro-tidal range < 10 cm). Consequently, short-term water level fluctuations are predominantly governed by stochastic atmospheric forcing, making "storm surges" the critical hazard for coastal management. This research specifically targets the Southern Caspian Basin, which encompasses the entire northern coastline of Iran. Physiographically, this basin represents the deepest sector of the sea, characterized by an oceanic-type crust and abyssal depths reaching approximately 1025 meters.

However, from the perspective of long-wave hydrodynamics and surge generation, the governing parameter is not the maximum abyssal depth, but rather the stark asymmetry in the continental shelf geometry and the variable width of the shallow coastal zone (nearshore hypsometry). The basin exhibits a pronounced morphological anisotropy; the western shelf is narrow and steep, rapidly dropping to deep water, whereas the eastern shelf is extensive and gently sloping. This morphological configuration interacts critically with the region's meteorology. The sea's significant meridional elongation (stretching over 1200 km from north to south) aligns perfectly with the dominant synoptic wind patterns.

During storm events, particularly in the cold season, high-velocity Northerly and North-Westerly winds sweep across the entire length of the sea. This alignment generates an exceptionally long "Effective Fetch" exceeding 800 km for the southern coast. This immense fetch facilitates the maximum transfer of momentum flux from the atmosphere to the sea surface, allowing wind-driven currents to accelerate over vast distances without topographic interruption. This process significantly enhances the potential for the generation of high-energy long waves and the mass transport of water towards the Iranian coast. Furthermore, the coastal topography in the southeastern sector (Gomishan and Gorgan Bay) functions as a "geometric funnel." In this region, the converging coastlines and the dissipative shallow bottom act to trap the incoming wind-driven currents. This "hydrodynamic confinement" prevents the lateral escape of the water mass, leading to a localized, non-linear amplification of surge heights that is significantly more severe than in the deep western sectors.

3.2. Morphological Classification and Hydrodynamic Characterization of Selected Stations

To ensure a rigorous hydrodynamic analysis that is spatially generalizable across the entire ~860 km southern coastline, six strategic monitoring stations

were selected based on distinct bathymetric gradients and socio-economic vulnerability profiles. The spatial configuration of these stations is visualized in Figure 1(a), while a comparative analysis of their cross-shore depth profiles is presented in Figure 1(b), revealing a pronounced east-west morphological asymmetry.

At the eastern extremity of the study domain, the Gomishan station serves as the archetype for the "Shallow Coastal Plain Regime." As delineated by the solid blue profile in Figure 1(b), this sector is characterized by an exceptionally gentle seabed gradient (slope S_0<1:1000), where shallow waters persist for significant distances offshore. From a theoretical fluid dynamics standpoint, this bathymetric configuration creates a friction-dominated environment. The governing momentum balance in this zone is heavily influenced by the bottom shear stress term (τ_b), which, combined with the inverse dependence of wind setup on water depth ($\partial\zeta/\partial x \propto \tau_s/h$), renders this region uniquely susceptible to extreme water level accumulation. Consequently, Gomishan serves as a critical indicator for "worst-case" inundation scenarios, where the synergy of low-lying topography and sustained storm winds creates a high-risk zone for extensive coastal flooding.

Moving westward, the central coastal sector-encompassing Amirabad Port, Neka, and Nowshahr exhibits a "Transitional Morphological Regime." This zone, which hosts vital energy and commercial infrastructure, features a bathymetric slope that represents an intermediate state between the dissipative east and the reflective west (Figure 1b). In this sector, the hydrodynamic focus shifts towards the interaction between the sea state and coastal structures; specifically, the determination of safe crest elevations for breakwaters against combined surge and wave run-up becomes paramount. Furthermore, the Nowshahr station presents a unique meteorological complexity; the immediate proximity of the Alborz Mountain range to the coastline induces localized orographic effects that modify the wind field structure, thereby increasing the complexity of the nearshore current generation.

Conversely, the western littoral zone, represented by Anzali Port and Astara, typifies the "Narrow Shelf Regime." In this region, bathymetric contours (isobaths) run parallel and in close proximity to the shoreline, indicating a steep seabed gradient as evidenced by the rapid depth descent in Figure 1(b) (dashed orange and solid purple lines). The fundamental nature of marine hazards in this sector is distinct from the east; while the amplitude of wind-induced surge is hydrodynamically constrained by the greater water depths, the steep slope allows high-energy, deep-water waves to propagate to the nearshore zone with minimal energy dissipation due to friction. Consequently, the primary engineering concern transitions from inundation to structural integrity, as coastal defenses are subjected to severe dynamic pressures and impulsive wave impact loads. Additionally, the hydrodynamics at Anzali are further complicated by the hydraulic exchange with the Anzali Lagoon and the interaction of inflow/outflow currents with port breakwaters. This strategic stratification of stations ensures a holistic coverage of the diverse hydrodynamic boundary conditions characterizing the Southern Caspian Sea.

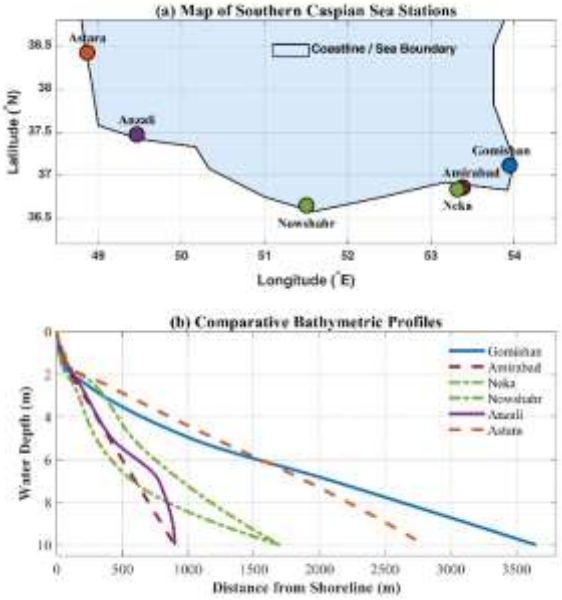

Figure 1: (a) Geographical map of the Southern Caspian Sea indicating the locations of the six selected study stations. The sea domain is highlighted in light blue, bounded by the coastline (solid black line). (b) Comparative cross-shore bathymetric profiles for the selected stations. The plots illustrate the significant morphological heterogeneity across the basin, contrasting the extremely gentle slope at Gomishan (solid blue line) with the steep gradients observed at Astara (dashed orange line) and Amirabad (dashed red line).

4. Results and Discussion

In this section, the complex hydrodynamic response of the Southern Caspian Basin to a spectrum of atmospheric forcing scenarios is critically examined through a rigorous quantitative analysis of the ADCIRC numerical model outputs. The discussion is structured to systematically unravel the physical mechanisms governing surge generation and propagation within this semi-enclosed water body. The analytical framework is founded on three primary axes designed to provide a holistic understanding of the basin's behavior. First, the study evaluates the non-linear damping and amplification effects induced by the basin's heterogeneous seabed morphology, specifically contrasting the dissipative, friction-dominated regime of the shallow southeastern shelf with the reflective nature of the deep western coast. Second, a decomposition analysis is performed to rigorously decouple the static, hydrostatic contribution of barometric pressure anomalies (Inverse Barometric

Effect) from the dynamic, momentum-driven wind shear stress, thereby isolating the dominant energy source responsible for extreme water levels. Finally, the investigation extends to the temporal dynamics of surge evolution relative to the wind field orientation, meticulously assessing how the effective fetch length and the angle of wave incidence interact with the basin's geometry to determine the magnitude, timing, and phase of the resulting storm surges.

4.1. The Role of Bathymetric Morphology in Non-linear Surge Amplification

A fundamental finding of this research is the elucidation of a distinct, non-linear inverse correlation between the nearshore water depth (h) and the amplitude of surge oscillations (ζ). The quantitative results, summarized in Table 1, reveal a severe spatial heterogeneity in the hydrodynamic response of the sea along the southern coastline. By isolating the critical "North-West Wind" scenario, the disparity in surge magnitudes becomes starkly evident. The Gomishan station, situated in the shallow southeastern coastal plain, recorded the highest surge level among all stations (5.88×10^{-2} m). In sharp contrast, at stations characterized by steep continental slopes and deep waters, such as Nowshahr and Anzali, this value diminishes significantly to 4.6×10^{-3} m and 4.7×10^{-3} m, respectively. This represents an order-of-magnitude difference—approximately a factor of 12—between the eastern and western sectors, despite both regions being subjected to identical wind forcing vectors.

The physical interpretation of this amplification phenomenon is rooted in the balance of momentum within the Shallow Water Equations (SWE), where the wind setup slope ($\partial\zeta/\partial x$) is inversely proportional to the total water depth. In the deep western regions like Astara, the large water depth results in a negligible surface gradient. Furthermore, in these deep waters, a vertical circulation cell is typically established where the wind-driven surface transport is effectively balanced by a deep "return flow" (undertow) driven by the pressure gradient, thereby preventing excessive water accumulation at the boundary. However, in the extensive shallow shelf of Gomishan, where depths remain below a few meters for significant offshore distances, the limited cross-sectional area restricts this return flow mechanism. Consequently, the turbulent bottom boundary layer expands to occupy the entire water column, drastically increasing the bottom friction stress (τ_b) and creating a "hydrodynamic impedance" that traps the water mass against the coast. With the return flow effectively choked, the kinetic energy of the wind-driven current cannot be dissipated through circulation and is almost entirely converted into potential energy, manifesting as a severe rise in the water surface. Thus, the seabed depth gradient serves as the primary controlling parameter determining the hydrodynamic regime, shifting the system from a diffusive, circulatory state in the west to a dissipative, accumulative state in the east.

4.2. Decoupling the Hydrostatic Atmospheric Pressure Contribution from Wind Shear Stress

In the complex hydrodynamics of enclosed basins, distinguishing the specific contribution of atmospheric pressure anomalies from the dominant wind shear stress is fundamental for accurate surge prediction. To rigorously quantify these relative contributions, the water level response to atmospheric pressure variations is meticulously analyzed in Figure 2. This comparative analysis examines the temporal evolution of the water surface under two distinct synoptic scenarios: a reference condition characterized by a standard pressure of 1025 hPa, and a storm condition defined by a cyclonic depression to 1020 hPa.

A detailed examination of the resultant time-series reveals that the imposed 5 hPa pressure deficit induces a nearly constant, vertical translation of the surge hydrograph across the entire simulation period. This uniform vertical shift is physically attributable to the sea's isostatic adjustment to the reduced weight of the atmospheric column, a phenomenon classically defined as the "Inverse Barometric Effect" (IBE). In accordance with the hydrostatic equilibrium principle, the sea surface rises approximately 1 centimeter for every 1 hPa drop in atmospheric pressure to balance the total pressure at the seabed. Consequently, the observed difference represents a static, scalar addition to the datum level rather than a dynamic generation of new wave energy.

Crucially, a closer inspection of Figure 2 demonstrates a high degree of "temporal phase synchronization" between the two scenarios. The onset time of the surge, the rate of rise, the exact moment of the peak, and the subsequent relaxation curve remain virtually invariant despite the pressure difference. This phase congruency provides compelling evidence that the system's dynamic characteristics—including flow inertia, wave celerity, and resonance frequencies—are dictated almost exclusively by the "Wind Stress Field." While the pressure anomaly modifies the potential energy of the system by elevating the mean water level, it does not significantly alter the kinetic energy transfer or the momentum balance within the basin. Therefore, in the context of coastal engineering for the Caspian Sea, atmospheric pressure functions primarily as a linear additive component, whereas the wind field acts as the vector driver determining the severity and temporal dynamics of the storm surge. This distinction is vital for design purposes, suggesting that while pressure drops must be accounted for in Total Water Level (TWL) calculations, the structural resilience against hydrodynamic impact loads must be designed based on wind-generated kinematics.

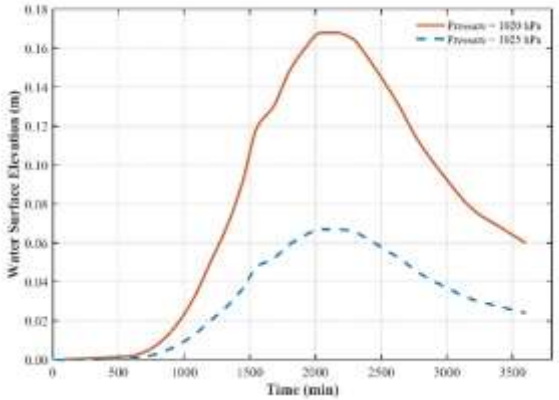

Figure 2: Time-series comparison of storm surge elevation under normal (1025 hPa) and storm (1020 hPa) atmospheric pressure scenarios.

4.3 Hydrodynamic Sensitivity to Wind Vector Orientation and Temporal Dynamics

The orientation of the wind stress vector relative to the basin's geometry serves as the governing determinant for the "Effective Fetch" length and the angle of wave incidence, which in turn dictates the magnitude of momentum transfer from the atmosphere to the sea surface. The sea surface response to Northerly winds, as plotted in Figure 3(a), illustrates a basin-wide setup phenomenon where the wind vector aligns perfectly with the longitudinal axis of the Caspian Sea. This alignment maximizes the effective fetch to over 800 km, facilitating a sustained transfer of momentum and allowing wind shear stress to act over a vast distance. Consequently, significant kinetic energy is converted into potential energy in the form of surge setup. A critical observation in this scenario is the spatial disparity in growth rates; the curve for the Gomishan station ascends with a significantly steeper gradient compared to deep-water stations. This behavior is attributed to the "shoaling effect," where long-period surge waves encounter the shallow continental shelf, decreasing in celerity but increasing in amplitude to conserve energy flux. Furthermore, the post-storm relaxation phase at Gomishan exhibits a noticeable hydrodynamic hysteresis; this delayed subsidence is attributable to the high bottom friction in the shallow, semi-enclosed region, which impedes the rapid drainage of the accumulated water mass back into the deep basin.

Conversely, the basin's response to lateral zonal forcing specifically Easterly Figure 3(e) and Westerly Figure 3(d) winds exhibits a fundamentally different, damped behavior. Due to the severe limitation of fetch length in the transverse direction, which is approximately 200 to 300 km, the wind lacks sufficient distance to generate a large hydraulic gradient or significant cross-shore setup. Instead, the hydrodynamics in these scenarios are governed by Ekman Transport. For instance, under Easterly winds, surface water is deflected to the right (Northward) due to the Coriolis effect, moving away from the Southern coast. Consequently, western stations like Anzali do not experience a rise and may even record a distinct "set-down" or negative surge. In these zonal scenarios, the generated currents acquire a predominantly "longshore" nature, dissipating storm energy by transporting water masses parallel to the coast rather than piling them up against the shoreline.

Table 1: Maximum storm surge elevation (*m*) calculated for selected stations under various wind direction scenarios.

Station	North (N)	North-West (NW)	North-East (NE)	West (W)	East (E)
Gomishan	0.0225	0.0588	0.0388	0.0670	0.0713
Amirabad	0.0108	0.0127	0.0071	0.0028	0.0028
Nowshahr	0.0107	0.0046	0.0041	0.0021	0.0022
Anzali	0.0116	0.0047	0.0075	0.0020	0.0020
Astara	0.0185	0.0150	0.0106	0.0190	0.0190

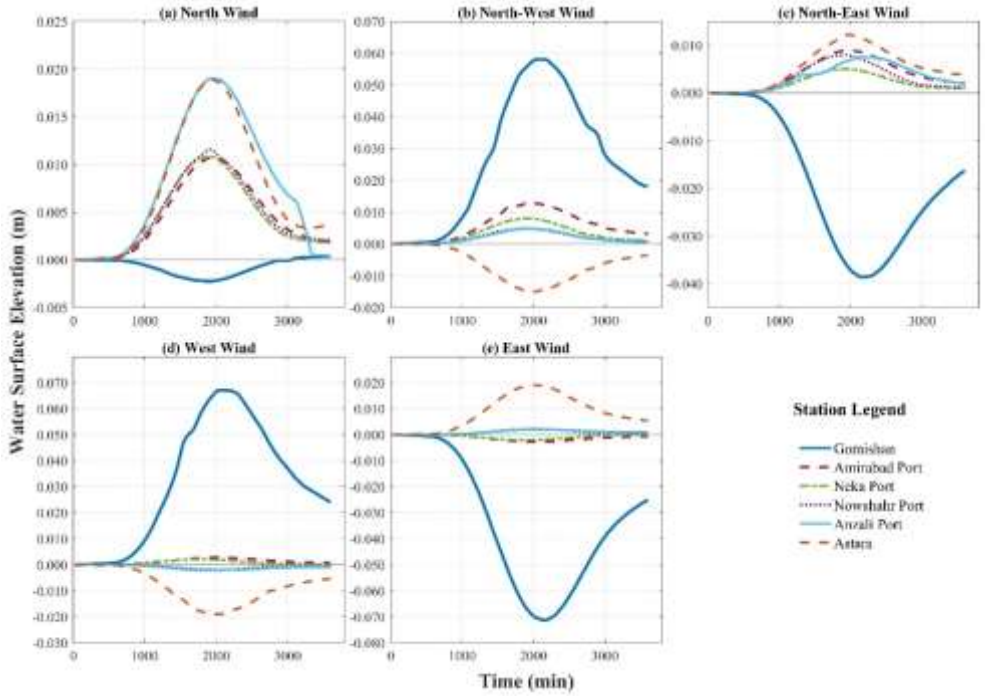

Figure 3: Multi-panel time series analysis of water surface elevation fluctuations across selected stations under five distinct wind direction scenarios (Wind Speed *U*=12 m/s). The subplots represent the hydrodynamic response to: (a) North, (b) North-West, (c) North-East, (d) West, and (e) East wind forcing. Panel (f) provides the unified legend for all stations. Note the scenario-specific vertical scales used to visualize the varying magnitudes of surge setup and set-down.

The interaction becomes more complex under oblique wind forcing. Examination of the North-East wind in Figure 3(c) reveals a nuanced mechanism involving both wind stress and the Coriolis force. The broad peak width observed in this graph indicates a sustained high-water stand. While the wind vector drives water toward the southwest, the Coriolis force deflects the flow to the right, effectively compressing the water mass against the Southern shoreline. This results in a "flow convergence" zone in the central parts of Mazandaran, which is evident in the overlapping curves of Amirabad and Nowshahr, creating a unique hazard profile for central ports. Finally, the most critical "Limit State" scenario is depicted in Figure 3(b) under North-West wind conditions. This graph represents the worst-case hydrodynamic loading for the southeastern sector, where the water level at Gomishan and Amirabad grows exponentially. The physical interpretation of this catastrophic event stems from the synergy of three destructive factors: the maximization of fetch along the sea's longest diagonal, the nearly orthogonal incidence of the wind relative to the bathymetric contours, and the "Momentum Trapping" caused by the funnel-shaped geometry of Gorgan Bay. In this state, the driven water mass encounters a closed boundary with no escape route, forcing a direct conversion of kinetic energy into a drastic vertical rise and posing an extreme risk of coastal flooding.

To synthesize the directional sensitivity results into a holistic framework, Figure 4 integrates the maximum surge responses from all simulated scenarios into a unified Polar Diagram. This synoptic visualization highlights a profound morphological disparity in hydrodynamic behavior across the study area. The Gomishan station, delineated by the expansive outer polygon, exhibits acute sensitivity to a broad spectrum of wind vectors, a phenomenon that can be termed the "Gomishan Anomaly." This empirically corroborates that in shallow hydrodynamic regimes, surge amplification is less constrained by the precise angle of wind incidence and is driven primarily by the sheer magnitude of bottom friction and shallow-water terms. In contrast, deep-water stations such as Nowshahr and Anzali form a constricted, compact core near the origin of the plot. Their response is highly anisotropic, reacting predominantly to direct Northerly forcing while remaining largely unresponsive to lateral winds. This behavior validates the energy-damping capacity of steep bathymetric slopes, which function as reflective boundaries. Collectively, the elongation of all station polygons towards the North and North-West sectors visually underscores these vectors as the determinant "Design Wind Directions" for the basin.

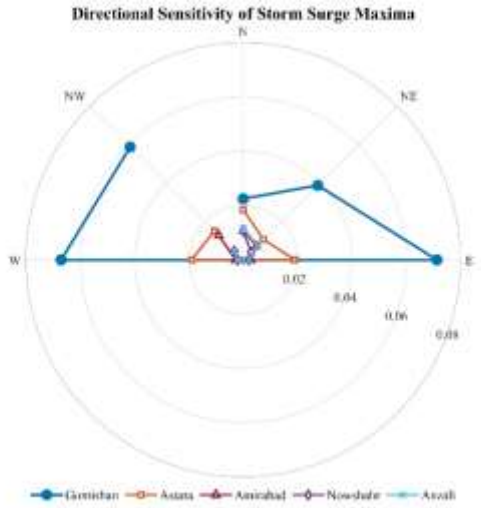

Figure 4: Polar diagram illustrating the directional sensitivity of maximum storm surge elevation across selected stations in the Southern Caspian Sea.

Finally, to quantify the "hydrodynamic stability" of different coastal sectors for reliability-based design, a statistical analysis of surge variability is presented in the Box-and-Whisker plot in Figure 5. This visualization reveals a critical distinction in risk profiles. The Gomishan station exhibits a significantly larger Interquartile Range (IQR) combined with a high median value, indicating that the region is not only subject to high water levels but is also highly volatile; the surge magnitude fluctuates wildly depending on slight shifts in the storm track. Conversely, stations in the central and western sectors show compact distributions with low medians, suggesting a stable hydrodynamic response where extreme surges are rare anomalies rather than frequent occurrences. This statistical evidence supports the engineering recommendation for implementing higher Safety Factors and more conservative freeboard allowances in the design of coastal structures in the southeastern Caspian basin compared to the western coast.

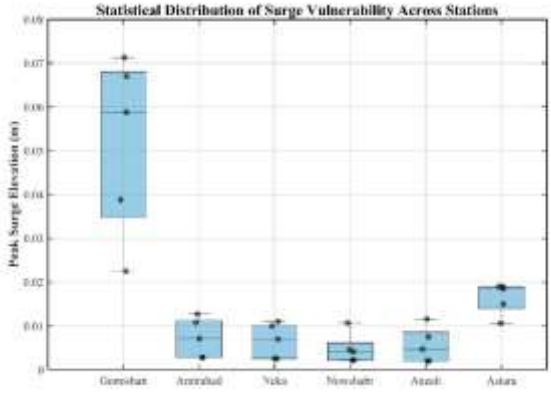

Figure 5: Statistical box-and-whisker plot illustrating the variability and distribution of peak surge elevations for each station across all simulated wind directions. The solid boxes represent the interquartile range (IQR), the red lines indicate the median surge, and the scattered points denote specific scenario outcomes.

4.4 Critical Scenario Analysis and Limit State Assessment

While historical records and long-term field observations suggest that the frequency of extreme storm surge events in the deep Southern Caspian Basin is lower compared to the shallow Northern sector, relying solely on average or moderate storm conditions ($U \approx 12$ m/s) is insufficient from the perspective of rigorous risk management and critical infrastructure design. In resilience engineering, defining a "Limit State" is essential to understand the structural behavior under "worst-case" scenarios that may occur within a 50 or 100-year return period. It is posited that analyzing a hypothetical "Critical Scenario" is indispensable to fully elucidate the basin's latent hydrodynamic potential, reveal hidden vulnerabilities in seemingly safe zones, and determine the upper bounds of Design Water Levels (DWL).

To this end, a comprehensive limit state scenario was constructed and simulated. This scenario is characterized by a sustained, high-velocity wind field of 25 m/s (classified as a severe storm in the Caspian region) combined with a barometric pressure depression to 1019 hPa. A "Westerly" wind vector was strategically selected as the critical forcing direction. This orientation is particularly hazardous because it aligns with the major East-West axis of the southern basin, maximizing the "effective fetch" for the southeastern coastline and driving strong Ekman transport currents directly toward the shallow Gomishan region.

4.4.1. Divergent Hydrodynamic Response

The simulation results under this extreme forcing, presented in Figure 6, reveal a drastic and highly non-linear bifurcation in the basin's hydrodynamic response. As illustrated, the water level at the Gomishan station undergoes a catastrophic escalation, experiencing a massive surge that reaches a peak of approximately +1.00 m. This phenomenon is not merely a linear increase but a result of "momentum trapping" within the funnel-shaped, shallow bathymetry of the southeastern corner, where bottom friction prevents the return flow of the piled-up water mass.

Conversely, the western sector exhibits a significant inverse response. The Astara station records a severe set-down (water level depression) of -0.59 m. Intermediate stations display a transitional behavior; Amirabad and Neka record moderate positive surges (~0.20–0.25 m), while centrally located stations like Nowshahr and Anzali experience water level drops of approximately 0.20 m. This profound divergence representing a nearly 1.6-meter hydraulic

gradient between the eastern and western coasts in a single event underscores the necessity for distinct, site-specific design strategies across the Southern Caspian littoral zone.

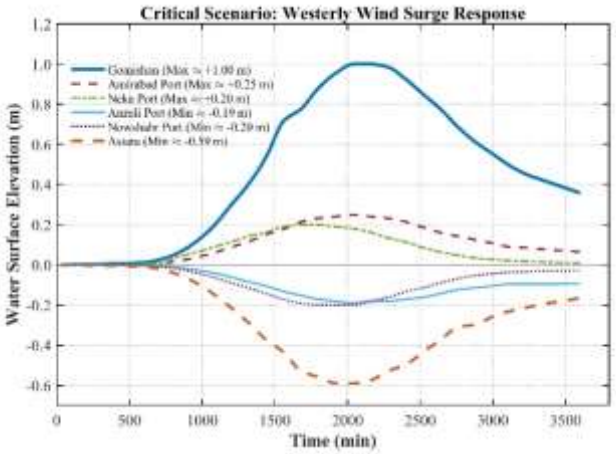

Figure 6: Hydrodynamic response simulation under the "Critical Limit State" scenario (Westerly wind, U=25 m/s, P_{atm}=1019 hPa). The graph highlights the extreme spatial heterogeneity, contrasting the massive surge setup at Gomishan (+1.0 m) with the significant set-down at Astara (−0.59 m).

4.4.2. Sensitivity and Amplification Analysis

To quantitatively assess the basin's sensitivity to wind stress intensification, Figure 7 presents a comparative "Dumbbell Plot." This advanced visualization illustrates the hydrodynamic shift from "Normal Conditions" (baseline, 12 m/s) to the "Critical Limit State" (25 m/s). In this chart, the vertical connector lines represent the magnitude of the surge shift, while the annotated values indicate the specific "Amplification Factor" calculated for each station. The analysis of these amplification factors yields critical engineering insights that challenge linear assumptions:

1. Severe Non-linearity: The approximate doubling of wind velocity (from 12 to 25 m/s) results in a disproportionate, non-linear surge response. At the critical Gomishan station, the surge elevation is amplified by a factor of approximately 15, escalating from negligible levels to a hazardous 1.00 m. This empirically validates the power-law dependence of wind stress ($\tau \propto U^2$) and its complex interaction with shallow water physics ($d \to 0$).
2. Unveiling Latent Vulnerability: A significant finding is the exceedingly high amplification factors observed in central and western deep-water stations (e.g., Anzali, Nowshahr, and Amirabad). Although these locations exhibit negligible fluctuations under normal forcing (indicated by blue markers near zero), the limit state simulation reveals their latent hydrodynamic potential. Under extreme stress, they experience significant hydraulic shifts (up to ±0.25 m). This underscores that the apparent "safety" of these deep-water zones under moderate winds must not lead to underestimating risks during high-return-period storms.
3. **Symmetry in Negative Response:** The Astara station exhibits a massive amplification factor (approx. 31x) for water level depression. This indicates that the physical mechanism driving water evacuation from the steep western coast operates with even greater intensity than the accumulation mechanism under extreme forcing, posing risks for navigation safety and water intake structures.

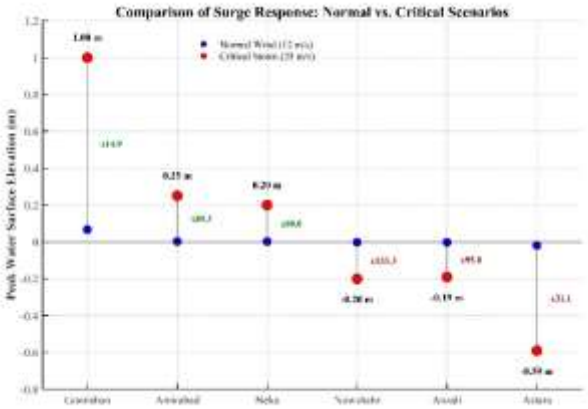

Figure 7: Comparative analysis of surge response sensitivity to wind velocity intensification. The chart illustrates the transition from the baseline scenario (12 m/s, blue markers) to the critical limit state (25 m/s, red markers). The calculated "Amplification Factors" (e.g., x14.9, x31.0) highlight the non-linear hydrodynamic response across all stations.

4.4.3. Basin-Scale Hydraulic Gradient

To visualize the holistic, basin-wide hydrodynamic response, the spatial distribution of the peak surge is plotted along the coastline in Figure 8. This profile reveals a coherent and continuous "Longitudinal Hydraulic Gradient" spanning approximately 850 km. The interplay between the sustained wind stress and the variable bathymetry creates a distinct "tilting" of the entire water surface in the Southern Caspian basin. The western sector (from Astara to Nowshahr) acts as a "source region" characterized by negative water levels (set-down zone), while the eastern sector functions as a "sink region," accumulating the displaced water mass. The pivotal point (hydrodynamic node or zero-crossing) is located in the central region between Nowshahr and Neka. This sharp gradient rising from -0.59 m in the west to +1.00 m in the east confirms that the storm surge in the Southern Caspian is not a localized event but a coupled, basin-scale oscillation (seiche-like behavior). This finding is crucial for integrated coastal zone management, as it implies that extreme events affect the entire coastline simultaneously but with opposing signs and magnitudes.

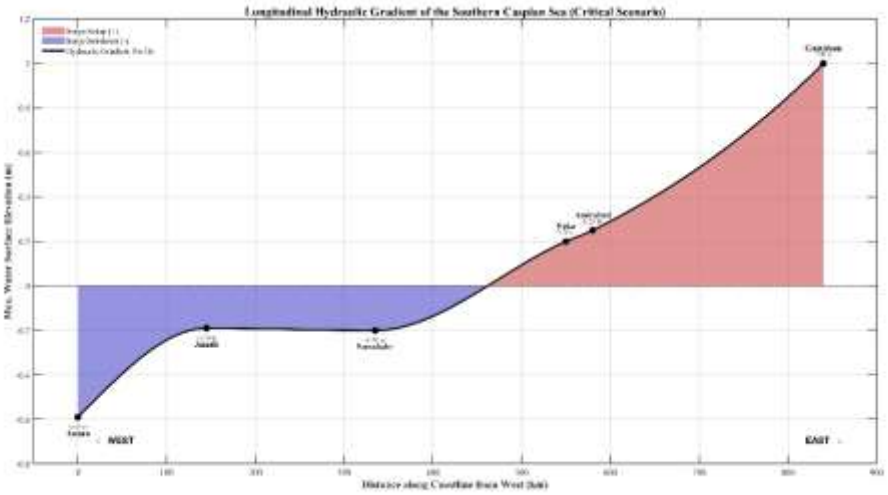

Figure 8: Longitudinal spatial profile of the maximum water surface elevation along the Southern Caspian coastline (from West to East) under the critical Westerly storm scenario (U=25 m/s). The plot visualizes the basin-scale "Hydraulic Gradient," illustrating the transition from significant set-down in the West (Astara) to extreme setup in the East (Gomishan).

5. Conclusion and Future Perspectives

This research constitutes a systematic effort to characterize the hydrodynamic response of the Southern Caspian Sea basin to extreme atmospheric forcing. By deploying the advanced, finite-element-based ADCIRC numerical model, this study successfully decoupled the complex, non-linear interactions governing storm surge generation, offering critical insights into the interplay between meteorological inputs and bathymetric controls. The comprehensive analysis of various synoptic scenarios yields the following pivotal conclusions and strategic recommendations:

5.1. Dominance of Wind Stress and Hydrodynamic Forcing

The simulation results provide conclusive evidence that within the semi-enclosed basin of the Caspian Sea, water level fluctuations during storm events are predominantly driven by the vector and magnitude of "wind shear stress" combined with the "effective fetch length." Unlike open oceanic environments where tidal constituents or barometric pressure drops often dictate peak water levels, in the Caspian Sea, the Inverse Barometric Effect plays a secondary, linear role, contributing only incrementally to the surge datum. Specifically, during the unstable transition seasons of autumn and winter, the alignment of high-velocity Northerly and North-Westerly wind fields with the sea's longitudinal axis facilitates a maximized momentum transfer from the atmosphere to the water column. This sustained energy input fosters the development of long-period surge waves that propagate southward, accumulating significant energy before impacting the Iranian coastline.

5.2. Bathymetric Control and Spatial Heterogeneity

A fundamental scientific contribution of this study is the quantitative elucidation of the critical role played by the "seabed gradient" in dictating the coastal hydrodynamic regime. The spatial analysis reveals a stark dichotomy in surge behavior:

- The "Hydrodynamic Trap" of the Southeast: The southeastern coastal zones, encompassing Gomishan and the Miankaleh peninsula, are characterized by a wide continental shelf, extremely shallow bathymetry, and a funnel-shaped coastal geometry. This configuration acts as a dissipative domain that effectively traps flow momentum. The high bottom friction in these shallow waters impedes the return flow, converting kinetic wind energy directly into potential energy, thereby generating severe surge setup and prolonged high-water stands.
- The Reflective Regime of the West: In sharp contrast, the western coasts (e.g., Anzali and Astara) feature steep bathymetric slopes and narrow shelves. These areas exhibit a reflective hydrodynamic behavior where deep-water waves reach the shoreline with minimal energy dissipation but limited potential for water pile-up. This severe spatial heterogeneity invalidates the use of a uniform "Design Water Level" (DWL) across the basin, necessitating a site-specific hazard zoning approach.

5.3. Implications for Marine Structural Design and Coastal Management

From an engineering perspective, the identified hydrodynamic distinctiveness mandates tailored design philosophies for the eastern and western sectors:

- Eastern Sector (Inundation Risk): In regions like the Amirabad Port and Gomishan, the primary threat is "coastal inundation and overtopping." Consequently, the design priority must focus on optimizing the crest elevation

(freeboard) of breakwaters and coastal dikes. Calculations must account for the superposition of the maximum storm surge, wave setup, and potential sea-level rise to ensure structural safety over a 50-year return period.

- Western/Central Sector (Structural Integrity): In areas like Nowshahr and Anzali, although the surge elevation is comparatively lower, the significant water depth at the toe of structures allows for the penetration of high-energy, non-breaking waves. Here, the primary hazards shift to "impulsive impact loads" and "toe scour." Design strategies must therefore prioritize the stability of armor units, the robustness of vertical seawalls against dynamic pressures, and the implementation of extensive scour protection measures.

5.4. Future Roadmap: Monitoring and Integrated Management

Finally, this study highlights an often-overlooked risk: the potential for resonance phenomena arising from the interaction between storm surges and infragravity waves (long waves) within harbor basins. It is strongly recommended that future research initiatives prioritize the establishment of a high-frequency field monitoring network. Synchronizing real-time water level registration with wave characteristics in identified critical zones (particularly the Gomishan anomaly) is essential for model calibration and early warning systems.

Furthermore, given the Caspian Sea's unique susceptibility to long-term sea-level fluctuations driven by climate change, the insights derived from this research should serve as a robust baseline for formulating Integrated Coastal Zone Management (ICZM) guidelines. These guidelines must establish conservative construction setbacks and define dynamic hazard lines to protect critical infrastructure and coastal communities against the compounding effects of extreme storms and sea-level variability.

References

Karami Khaniki, A. (2006). *Coasts of Iran*. Soil Conservation and Watershed Management Research Institute, Tehran, Iran (in Persian).

Luettich, R.A., & Westerink, J.J. (2004). *Formulation and numerical implementation of the 2D/3D ADCIRC finite element model version 44.xx*. Theory Report. Available at: <www.adcirc.org>.

Mahdizadeh, M. (2004). Numerical modeling of storm and wind-driven currents in the Caspian Sea. *Journal of Marine Sciences*, (in Persian).

Williams, A.E. (1986). *Engineering and design: Storm surge analysis and design water level determinations* (EM 1110-2-1412). Washington, D.C.: U.S. Army Corps of Engineers.

Wu, J. (1982). Wind-stress coefficients over sea surface from breeze to hurricane. *Journal of Geophysical Research: Oceans*, 87(C12), 9704–9706.

Yan, Y. (1987). *Numerical modeling of current and wave interactions of an inlet-beach system* (Doctoral dissertation). University of Florida, Gainesville, FL.